VIA MEDICA

ORIGINAL ARTICLE

Folia Morphologica
2026; 85: e01726036
DOI: 10.5603/fm.104428
© 2026 Via Medica
ISSN 0015–5659, eISSN 1644–3284
journals.viamedica.pl

Morphometric analysis and typing of talus and calcaneus bones from the Eastern Anatolian population

Asli Beril Karakas[1], Yalcin Akbulut[2], Burhan Yarar[3], Mukadder Sunar[4]

[1]Department of Anatomy, Kastamonu University, Faculty of Medicine, Kastamonu, Turkiye
[2]Department of Anatomy, Kafkas University, Faculty of Medicine, Kars, Turkiye
[3]Department of Anatomy, Ataturk University, Faculty of Medicine, Erzurum, Turkiye
[4]Department of Anatomy, Erzincan Binali Yıldırım University, Faculty of Medicine, Erzincan, Turkiye

[Received: 9 January 2025 Accepted: 29 April 2025 Published: 7 May 2025]

Background: *The talus and calcaneus are critical components of foot biomechanics, contributing to stability and movement. Despite their importance, data on their morphometric and articular characteristics in the Eastern Anatolian population are scarce. This study aimed to address this gap by analyzing the morphometry and facet configurations of the talus and calcaneus in this region and highlighting their clinical and biomechanical significance.*

Materials and methods: *A total of 32 tali and 29 calcanei were analyzed using high-resolution computed tomography (CT) and 3D reconstruction. Morphometric measurements, including lengths, widths, and facet areas, were performed, and articular facet types were classified based on established criteria. Comparative analyses were conducted with data from other populations.*

Results: *Side-specific variations were observed in lengths and sulcus dimensions. Type B was the most prevalent facet configuration in both the talus and calcaneus, with unique patterns such as Type B3 emphasizing the anatomical distinctiveness of the Eastern Anatolian population. Comparisons with other populations revealed larger morphometric dimensions and distinct facet distributions, underscoring population-specific differences.*

Conclusions: *This study provides valuable morphometric and facet classification data for the talus and calcaneus in the Eastern Anatolian population. These findings contribute to a deeper understanding of regional anatomical variations and have significant implications for clinical applications, forensic investigations, and prosthetic design.* (Folia Morphol 2026; 85: e01726036)

Keywords: 3D reconstruction; calcaneus; Eastern Anatolian population; facet typing; morphometry; population-specific anatomy; talus

INTRODUCTION

The talus and calcaneus are fundamental to weight-bearing, balance, and locomotion, playing a pivotal role in foot and ankle biomechanics [3]. Understanding their morphometric characteristics is crucial for surgical planning, prosthesis design, and fracture management [12, 41].

The calcaneus, as the largest tarsal bone, supports the posterior foot arch, while the talus facilitates ankle joint mobility [12, 40]. Morphometric parameters

Address for correspondence: Asli Beril Karakas, Department of Anatomy, Faculty of Medicine Kastamonu University, Kuzeykent Mahallesi, Orgeneral Atilla Ateş Paşa Caddesi No: 19, 37150 Merkez, Kastamonu, Turkiye; tel. +90 5069262503, e-mail: asliberilkarakas@gmail.com

This article is available in open access under Creative Common Attribution-Non-Commercial-No Derivatives 4.0 International (CC BY-NC-ND 4.0) licese, allowing to download articles and share them with others as long as they credit the authors and the publisher, but without permission to change them in any way or use them commercially.

such as Böhler's and Gissane's angles are critical in diagnosing calcaneal fractures and subtalar joint stability [31]. Variations in talocalcaneal joint morphology influence subtalar instability and degenerative changes, affecting clinical outcomes [20, 40].

Despite their clinical significance, the morphometric characteristics of the Eastern Anatolian population remain underexplored, necessitating population-specific data to optimize orthopedic, forensic, and rehabilitative applications. The aim of this study was to analyze talar and calcaneal morphology in this population, classify the articular facets, and examine their implications for joint function and clinical practice.

MATERIALS AND METHODS

Sample selection

This study analyzed 32 tali (16 right, 16 left) and 29 calcanei (17 right, 12 left) obtained from the Anatomy Departments of Kafkas University, Atatürk University, and Erzincan Binali Yıldırım University. The bones were of unknown age and sex. Only intact specimens were included, while those with fractures, deformities, or visible damage were excluded to ensure accurate morphometric assessments. Additionally, no information was available regarding whether the bones belonged to the same or to different individuals. The bones were treated as contemporary specimens for the purposes of this anatomical analysis. Their exact chronological origin could not be determined; however, no historical or archaeological designation was present, and all procedures adhered to ethical guidelines for anatomical research.

Ethical approval was obtained from the Atatürk University Ethics Committee, and all procedures adhered to the Declaration of Helsinki and institutional research guidelines.

Imaging and 3D model reconstruction

For classification purposes, each bone was photographed and subjected to computed tomography (CT) scanning with a slice thickness of 0.625 mm at the Kafkas University Training and Research Hospital. The acquired cross-sectional DICOM images were imported into 3D Slicer software (v. 5.6.1) for segmentation and morphometric analysis.

The segmentation process was performed by an experienced anatomist with more than 10 years of expertise (ABK), using both semi-automated and manual refinement techniques to ensure high anatomical accuracy (Fig. 1–4). The segmentation and measurement procedures were based on standardized anatomical protocols validated in previous studies [7, 42].

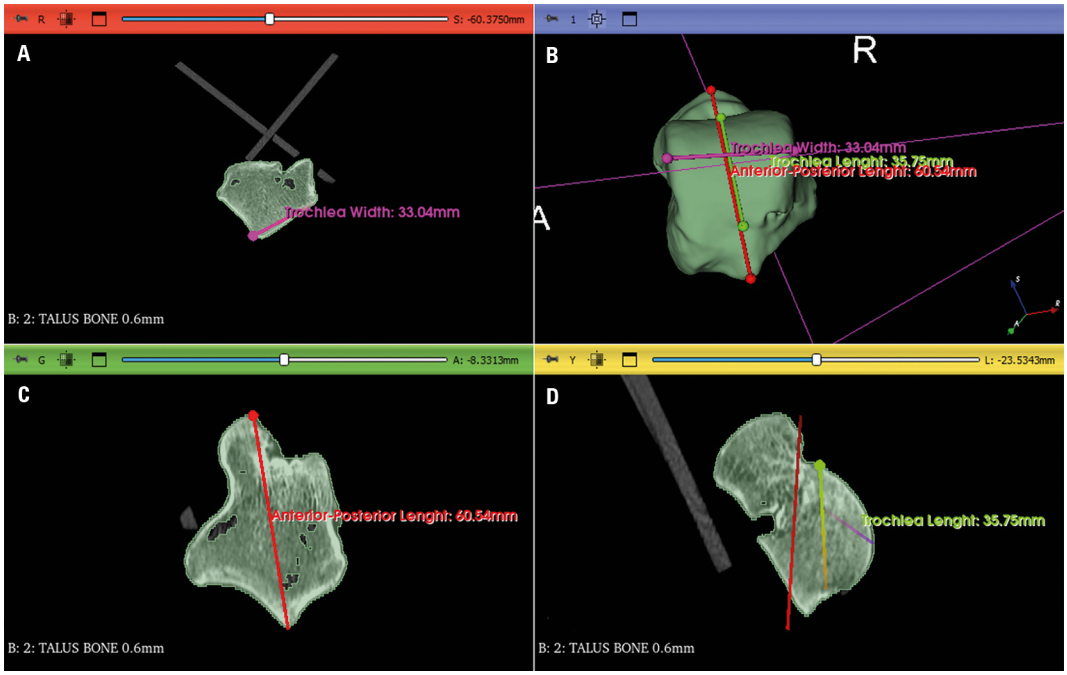


Figure 1. Different views illustrating the measurement methods of talus parameters, including trochlear width, trochlear length, and anterior--posterior length; **A.** The coronal section depicts the anterior-posterior length of the talus; **B.** The sagittal section shows the trochlear length of the talus; **C.** The axial section demonstrates the trochlear width of the talus; **D.** The 3D view visualizes the trochlear width, trochlear length, and anterior-posterior length parameters of the talus.

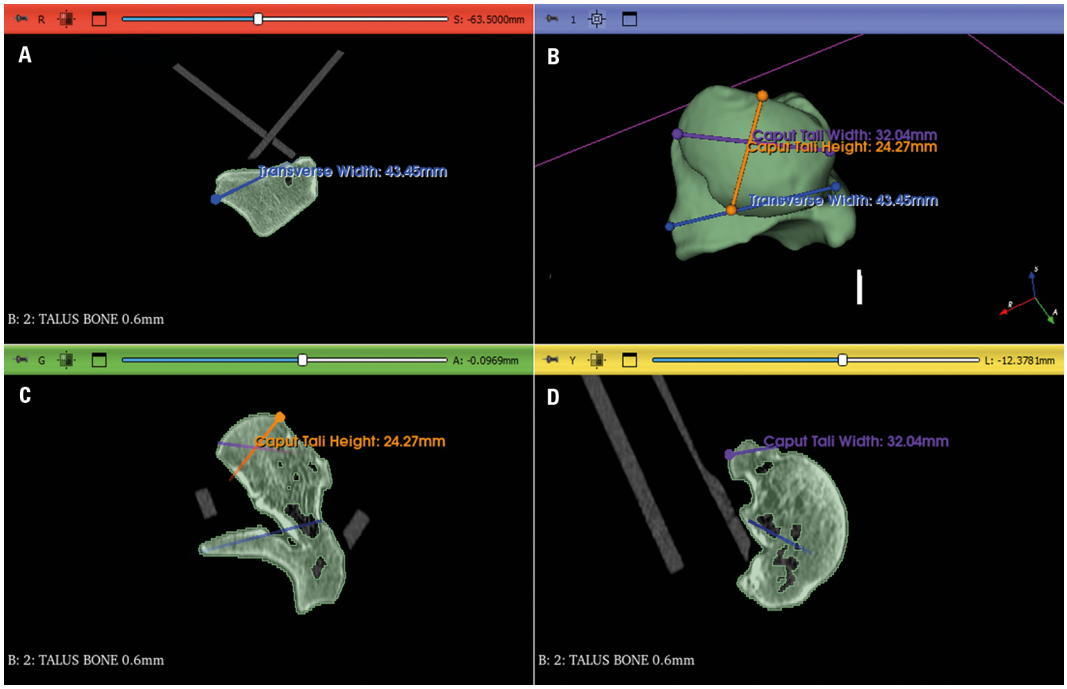


Figure 2. Different views illustrating the measurement methods of talus parameters, including caput tali height, caput tali width, and transverse width; **A.** The coronal section depicts the caput tali height of the talus; **B.** The sagittal section shows the caput tali width of the talus; **C.** The axial section demonstrates the transverse width of the talus; **D.** The 3D view visualizes the caput tali height, caput tali width, and transverse width parameters of the talus.

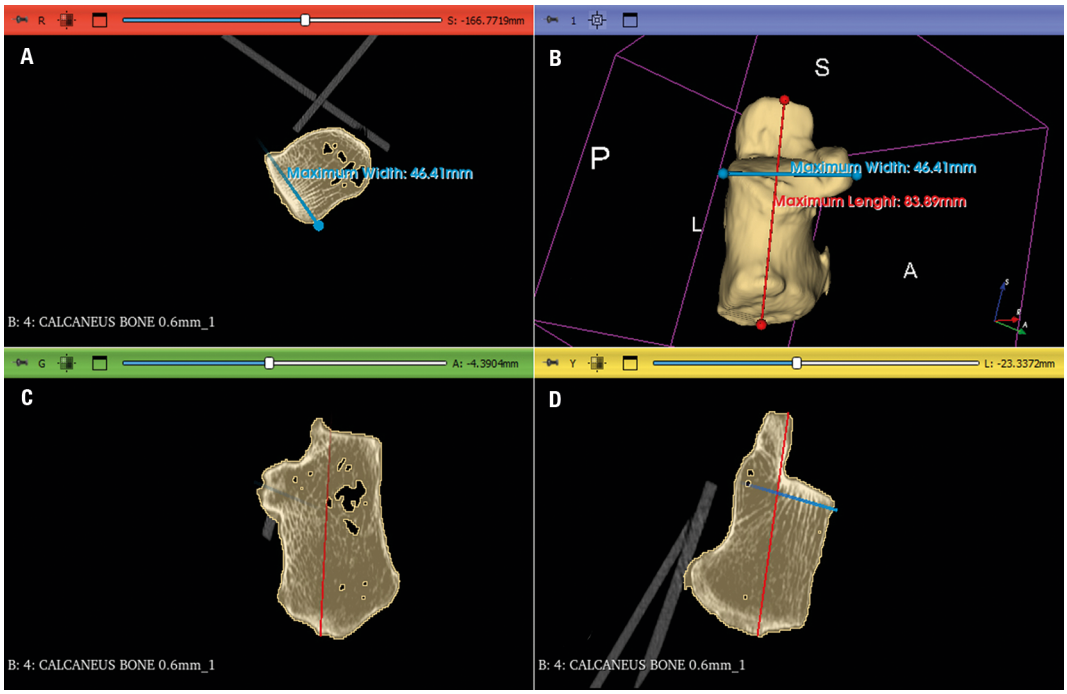


Figure 3. Different views illustrating the measurement methods of calcaneus parameters, including maximum length and maximum width; **A.** The coronal section depicts the maximum length of the calcaneus; **B.** The sagittal section shows the maximum length and maximum width of the calcaneus; **C.** The axial section demonstrates the maximum width of the calcaneus; **D.** The 3D view visualizes the maximum length and maximum width parameters of the calcaneus.

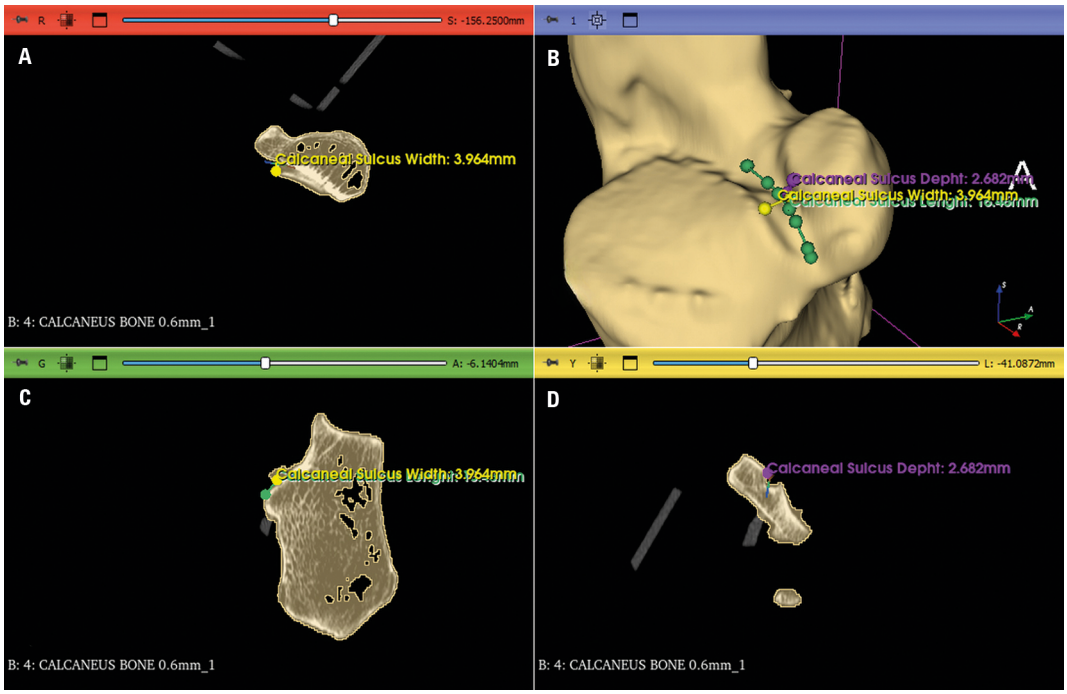


Figure 4. Different views illustrating the measurement methods of calcaneus parameters, including calcaneal sulcus width, depth, and length; **A.** The coronal section depicts the calcaneal sulcus width of the calcaneus; **B.** The sagittal section shows the calcaneal sulcus depth of the calcaneus; **C.** The axial section demonstrates the calcaneal sulcus width of the calcaneus; **D.** The 3D view visualizes the calcaneal sulcus width, calcaneal sulcus depth, and calcaneal sulcus length parameters of the calcaneus.

Segmentation and measurement protocol

Image preprocessing:

- The DICOM images were imported into 3D Slicer (v5.6.1).
- A Gaussian filter was applied to reduce noise while preserving edge details.
- Image contrast and brightness were adjusted to enhance bone-tissue differentiation.

Bone segmentation:

- Threshold-based segmentation was applied to isolate bone structures, using predefined Hounsfield Unit (HU) ranges for cortical and trabecular bone.
- The GrowCut algorithm, a region-growing segmentation method within 3D Slicer, was used to refine bone contours.
- Manual corrections were performed when necessary, ensuring alignment with anatomical landmarks.

3D model reconstruction:

- Segmented bone structures were converted into 3D surface models for morphometric analysis.
- The models were visually inspected and validated against original CT slices to ensure anatomical accuracy.

Morphometric measurement protocol:

- Morphometric measurements were performed using the Ruler and Angle tools in 3D Slicer, following established guidelines for bone morphometry.

The following key parameters were recorded:

- Maximum length, width, and height of the talus and calcaneus.
- The articular facet areas were measured using the Closed Curve tool within the Markups module of 3D Slicer, which provides automatic surface area calculation functionality. Fiducial points were manually placed along the anatomical margins of each facet to create closed curves delineating the surface boundaries.
- The enclosed surface areas were automatically computed by the software and expressed in square millimeters (mm^2).
- Böhler and Gissane angles, measured between pre-defined anatomical landmarks.

Validation and reliability:

- All measurements were conducted according to standard protocols to ensure accuracy and consistency.

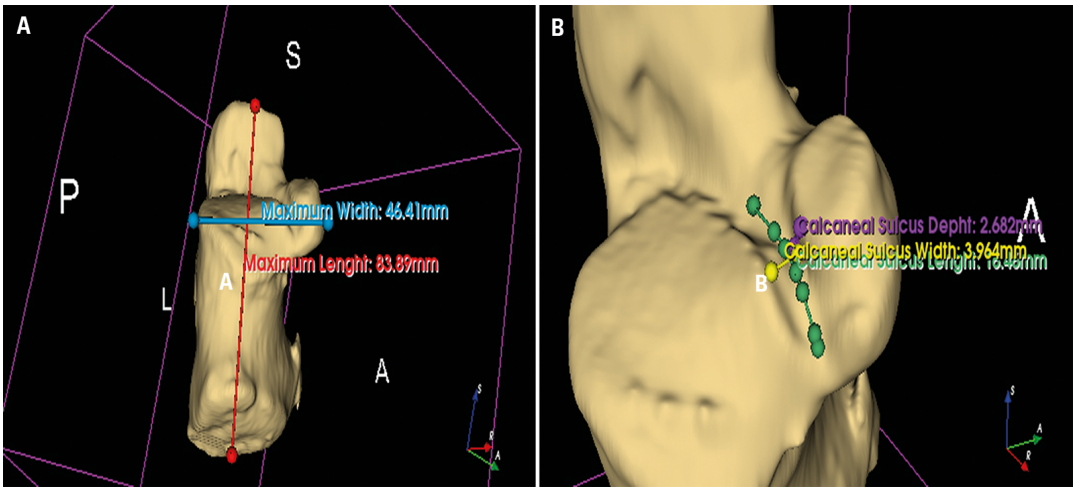


Figure 5. Detailed three-dimensional view of all parameters of the calcaneus; **A.** The 3D reconstruction image demonstrates the maximum length and maximum width parameters of the calcaneus; **B.** The detailed 3D reconstruction image demonstrates the calcaneal sulcus width, calcaneal sulcus depth, and calcaneal sulcus length parameters of the calcaneus.

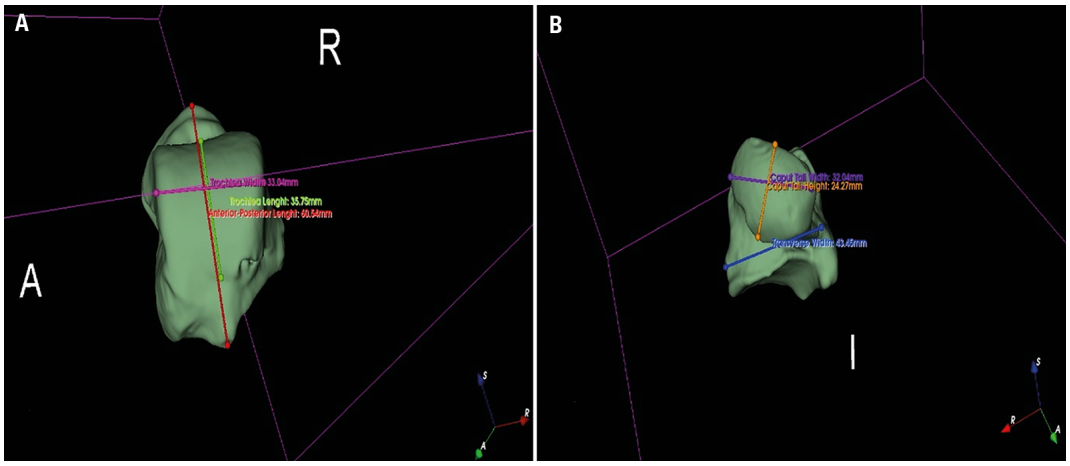


Figure 6. Detailed three-dimensional view of all parameters of the talus; **A.** The 3D reconstruction image demonstrates the trochlear width, trochlear length, and anterior-posterior length parameters of the talus; **B.** The 3D reconstruction image demonstrates the caput tali width, caput tali height, and transverse width parameters of the talus.

- Previous studies have demonstrated that 3D Slicer-based morphometric measurements are highly accurate and reproducible [7, 42].
- The methodology used in this study aligns with validated segmentation and measurement techniques, minimizing potential variability [15, 30].

Morphometric parameters

The following morphometric parameters were evaluated for the talus and calcaneus. Definitions are briefly summarized below, and the measurement methods are illustrated in Figures 1–6.

Talus

Trochlear measurements: trochlear length (TL) — maximum anteroposterior length, and trochlear width (TW) — maximum transverse width of the trochlear surface.

Caput tali measurements: caput tali height (CTH) — vertical height, and caput tali width (CTW) — maximum width of the talar head.

Overall dimensions of the talus: anterior–posterior length (APL) — maximum distance from the anterior to the posterior end, and transverse width (TW) — maximum mediolateral width.

Sulcus tali measurements: sulcus tali length (SL) — longitudinal length, Sulcus Tali Width (SW) — transverse width, and sulcus tali depth (SD) — maximum depth.

Articular facet areas: surface areas of the anterior, middle, and posterior facets.

Calcaneus

Angular measurements: Gissane angle (GA) — angle formed between the posterior facet and the slope of the calcaneus, and Böhler angle (BA) — angle between two tangent lines drawn to the anterior and posterior articular facets.

Overall dimensions of the calcaneus: maximum length (MCL) — anteroposterior length, and maximum width (MCW) — transverse width.

Sulcus calcanei measurements: Sulcus calcanei length (SL) — longitudinal length, Sulcus calcanei width (SW) — transverse width, and Sulcus calcanei depth (SD) — maximum depth.

Articular facet areas: surface areas of the anterior, middle, and posterior facets.

Facet typing

The classification of talar and calcaneal articular facets was performed following established morphological criteria from the literature [34].

Although multiple classification systems exist for facet typing, this method was selected because of its unique combination of anatomical precision, quantitative measurement criteria, and clinical applicability. The facet classifications proposed by Bunning and Barnett [4], Campos and Pellico [5], Madhavi et al. [29], Kori et al. [27], and Jung et al. [21] have provided valuable insights; however, most of these systems relied on qualitative observations rather than quantitative morphological criteria, leading to observer-dependent variability.

Prasad and Rajasekhar's classification overcomes many of the limitations observed in previous studies by integrating interfacet distances as a key parameter, allowing for a more objective and reproducible approach. Unlike earlier systems that primarily focused on the presence or absence of facet separation, this classification refines traditional morphological categorizations by incorporating additional facet subtypes. These refinements make the system particularly useful for anatomical and biomechanical research, as it enables a more precise differentiation of anatomical variations that may influence subtalar joint mechanics and stability. Additionally, this classification framework builds upon earlier models by structuring facet subtypes in a way that aligns with their functional and biomechanical significance. This is particularly important given that previous studies have noted a gap between anatomical classifications and their relevance in clinical practice.

One of the major limitations of traditional facet classification methods is their limited applicability to clinical and surgical settings. Many previous systems do not account for the biomechanical implications of different facet arrangements, which can influence weight distribution and stability within the subtalar joint. Prasad and Rajasekhar's approach incorporates these aspects, making it highly relevant to orthopedic and biomechanical research. Cockerill et al. [8] emphasized the importance of classification systems that bridge the gap between anatomical variation and clinical interpretation. By integrating measurable interfacet distances and structured subtypes, this system contributes to a more standardized and functionally meaningful classification of subtalar facets.

Therefore, in this study, subtypes were classified based on specific interfacet distances and morphological distinctions (Tab. 1) to ensure a structured and reproducible approach to subtalar facet variation.

Statistical analysis

All statistical analyses were performed using IBM SPSS Statistics (version 25.0). To ensure the reliability and reproducibility of the morphometric measurements for both the calcaneus and talus, all measurements were performed by a single anatomist. Descriptive statistics, including mean, standard deviation, minimum, and maximum values, were initially calculated for each morphometric parameter. To assess the distribution of the data, the Shapiro–Wilk test was applied, as it is particularly suitable for small sample sizes.

Based on the normality results, appropriate statistical tests were selected to compare morphometric measurements between the right and left sides of the talus and calcaneus. For normally distributed data, independent samples *t*-tests were performed, with Levene's test conducted beforehand to determine whether equal variances could be assumed. For non-normally distributed data, the Mann–Whitney U test was employed as a non-parametric alternative.

Table 1. Classification of talus and calcaneus facet types.

Type	Subtype	Description
A	A1	< 2 mm distance between anterior and middle facets, indicating a near-continuous articular surface.
	A2	2–5 mm distance between anterior and middle facets, suggesting partial separation with functional continuity.
	A3	> 5 mm distance between anterior and middle facets, signifying distinct and separate facet structures.
B	B1	Fused anterior-middle facets with smooth transitions, forming a single continuous articular surface.
	B2	Partially fused anterior-middle facets with a visible but incomplete separation between them.
	B3	Anterior articular facet absent, with the middle facet fully developed and positioned on the sustentaculum tali.
C	C1	Fully separate anterior, middle, and posterior facets, indicating complete segmentation of articular surfaces.
	C2	Separate facets with significant size differences, contributing to distinct variations in subtalar joint mechanics.

To further enhance the interpretability of the findings, effect sizes were calculated. Cohen's d was reported for normally distributed parameters analyzed with *t*-tests, while the rank-biserial correlation (r) was used for non-normally distributed parameters analyzed with the Mann-Whitney U test. Additionally, 95% confidence intervals (CIs) were determined for the mean differences in *t*-tests and the Hodges–Lehmann estimates in Mann–Whitney U tests to provide an interval-based interpretation of the results.

In addition to group comparisons, correlation analyses were conducted to explore potential associations between different morphometric parameters. Pearson's correlation coefficient was applied for normally distributed parameters, while Spearman's rank correlation was used for non-normally distributed parameters. Additionally, for correlations between a normally distributed and a non-normally distributed variable, Spearman's correlation was used to account for differences in data distribution.

The results were evaluated to identify structural patterns and their potential clinical significance in understanding joint stability and biomechanics.

RESULTS

This study evaluated 32 tali and 29 calcanei, focusing on morphometric parameters and facet typing. The mean morphometric values for both bones are summarized in Figures 7 and 8, including differences between the right and left sides.

Morphometric findings

Calcaneus measurements

Key morphometric parameters of the calcaneus are presented in Tables 2 and 3, and these parameters are shown in Figure 5.

- Gissane angle (GA): The mean GA was 135.92 ± ± 6.94° (range: 122.27–143.78°) on the right and 130.27 ± 7.72° (range: 120.89–142.08°) on the left. While the difference was not statistically significant ($p = 0.063$, $r = –0.345$), a trend toward lateral asymmetry was observed and should be interpreted with caution given the small sample size.
- Böhler Angle (BA): The mean BA was 37.28 ± ± 8.89° (range: 23.70–51.37°) on the right and 37.80 ± 8.35° (range: 21.70–52.88°) on the left ($p = 0.929$, $d = –0.061$, 95% CI: –7.23 to 6.19). A reduced BA is commonly associated with calcaneal fractures.
- Maximum length (MCL): The left calcaneus was slightly longer (94.13 ± 10.36 mm) than the right (89.44 ± 15.29 mm), though the difference was not statistically significant ($p = 0.565$, $d = –0.364$, 95% CI: –15.14 to 5.75). This parameter plays a crucial role in Achilles tendon function.
- Maximum width (MCW): The mean width was greater on the left (55.89 ± 5.34 mm) than on the right (50.75 ± 8.10 mm), with a p-value of 0.092 and an effect size of $r = –0.312$. Although this difference did not reach statistical significance, the effect size suggests a mild lateral asymmetry, potentially reflecting structural adaptations in weight distribution.
- Calcaneal sulcus dimensions: No significant differences were observed between sides in sulcus length, width, or depth ($p > 0.05$). The sulcus is essential for subtalar joint stability.
- Articular facet areas: The left side had slightly larger facet areas, which may influence weight-bearing and joint congruency, though these differences were not statistically significant ($p > 0.05$, $r = –0.173$ to $–0.066$).

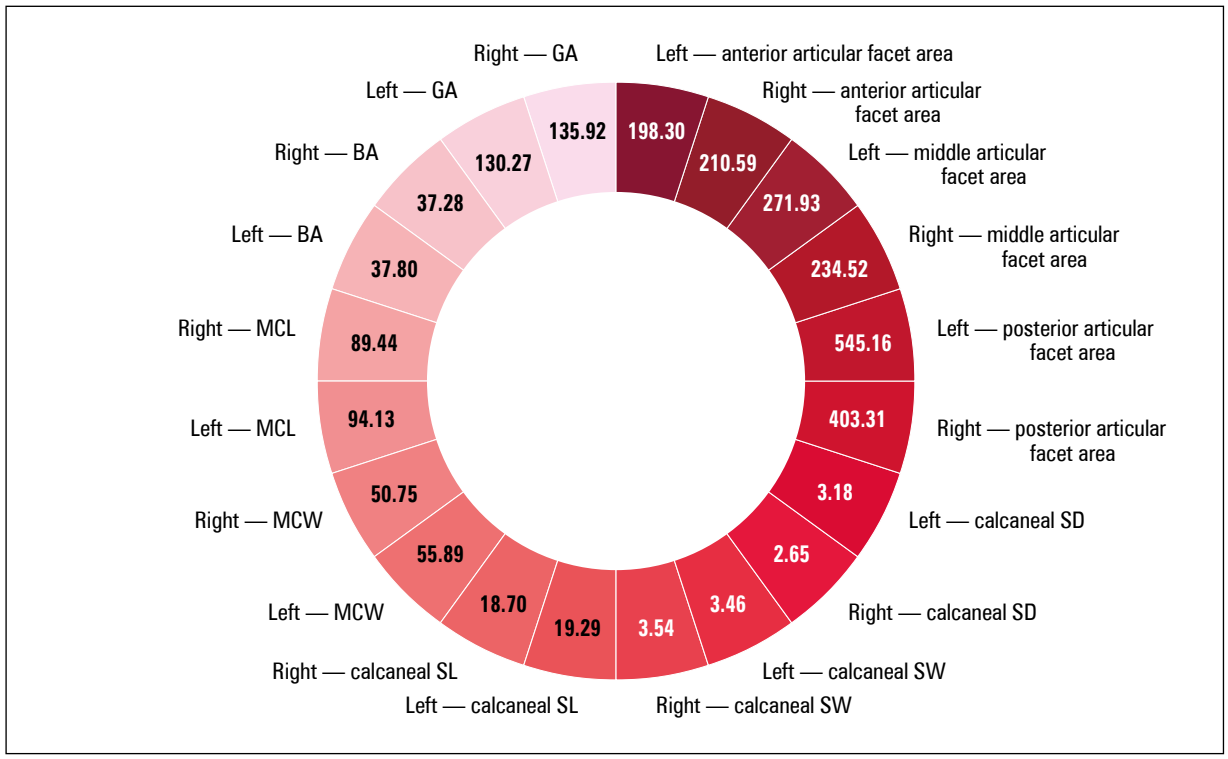


Figure 7. Circular visualization of calcaneus morphometric parameters between right and left sides. This circular plot displays the mean values of Gissane angle (GA), Böhler angle (BA), maximum length (MCL), maximum width (MCW), calcaneal sulcus length (SL), width (SW), depth (SD), and articular facet areas (posterior, middle, anterior) for the calcaneus, highlighting variations between the right and left sides.

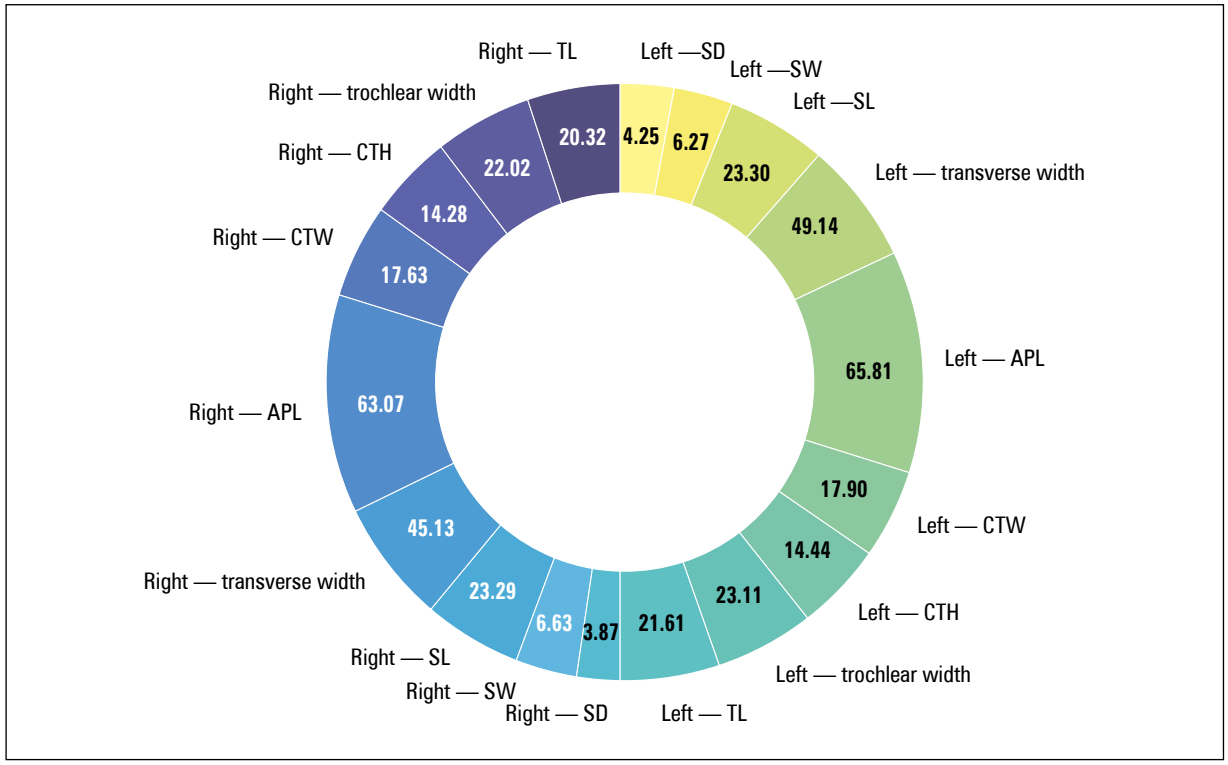


Figure 8. Circular visualization of talus morphometric parameters between right and left sides. This circular plot represents the mean values of trochlear length (TL), trochlear width, caput tali height (CTH), caput tali width (CTW), anterior-posterior length (APL), transverse width, and sulcus dimensions [length (SL), width (SW), depth (SD)] for the talus, demonstrating differences between the right and left sides.

Table 2. Morphometric measurements of the calcaneus between right and left sides.

Parameters	Side	N	Mean	SD	Min	Max	p	r/ Cohen's d	95% CI
GA	R	17	135.92	6.94	122.27	143.78	0.063	–0.345	(–2.100 to 19.300)
GA	L	12	130.27	7.72	120.89	142.08			
BA	R	17	37.28	8.89	23.70	51.37	0.929	–0.061	(–7.230 to 6.190)
BA	L	12	37.80	8.35	21.70	52.88			
MCL	R	17	89.44	15.29	58.98	106.95	0.565	–0.364	(–15.140 to 5.750)
MCL	L	12	94.13	10.36	77.90	110.89			
MCW	R	17	50.75	8.10	35.40	61.88	0.092	–0.312	(–1.500 to 10.200)
MCW	L	12	55.89	5.34	43.80	62.47			
SL	R	17	18.70	6.53	9.63	30.82	0.626	–0.099	(–5.467 to 4.284)
SL	L	12	19.29	5.97	9.92	28.64			
SW	R	17	3.54	1.58	1.89	8.16	0.507	–0.123	(–0.900 to 3.500)
SW	L	12	3.46	1.14	1.26	4.92			
Sulcus calcanei depth	R	17	2.65	1.16	0.93	5.32	0.232	–0.447	(–1.465 to 0.410)
Sulcus calcanei depth	L	12	3.18	1.29	0.95	5.11			
Posterior articular facet area	R	17	403.31	294.98	163.77	1100.59	0.352	–0.173	(–38.600 to 79.400)
Posterior articular facet area	L	12	545.16	332.96	96.20	1053.24			
Middle articular facet area	R	15	234.52	132.27	85.31	579.88	0.723	–0.066	(–15.200 to 33.500)
Middle articular facet area	L	8	271.93	170.82	62.30	537.39			
Anterior articular facet area	R	9	210.59	66.99	134.96	353.03	0.723	–0.066	(–12.800 to 23.600)
Anterior articular facet area	L	5	198.30	95.35	24.87	431.90			

BA — Böhler angle; CI — confidence interval; GA — Gissane angle; L — left; Max — maximum; MCL — maximum length; MCW — maximum width; Min — minimum; N — sample size; R — right; r — effect size; SD — standard deviation; SL — sulcus calcanei length; SW — sulcus calcanei width.

Table 3. Overall morphometric measurements of the calcaneus.

Parameter	Mean	SD	Min	Max	N
Trochlear length	20.97	7.86	10.04	40.51	32
Trochlear width	22.56	8.78	13.02	49.87	32
Caput tali height	14.36	5.09	9.05	28.13	32
Caput tali width	17.76	5.52	11.01	38.11	32
Anterior-posterior length	64.44	9.77	49.40	85.57	32
Transverse width	47.14	6.77	32.98	58.60	32
Sulcus tali length	23.29	3.79	16.30	30.69	32
Sulcus tali width	6.45	1.64	3.30	9.62	32
Sulcus tali depth	4.06	0.91	2.35	5.88	32
Anterior articular facet area	199.63	117.47	57.35	745.27	19
Middle articular facet area	337.43	183.63	48.73	1103.09	22
Posterior articular facet area	916.13	184.55	604.92	1288.61	32

Max — maximum; Min — minimum; SD — standard deviation.

Cohen's d values indicated negligible to small effect sizes, with the highest value observed for Maximum length (d = –0.364, 95% CI: –15.14 to 5.75), followed by Sulcus Calcanei Depth (d = –0.447, 95% CI: –1.46 to 0.41). However, all confidence intervals included zero, indicating that these differences were not statistically meaningful. Rank-biserial correlation (r) values derived from the Mann–Whitney U test supported these findings, with small to negligible effect sizes across all parameters (e.g., Gissane Angle r = –0.345, Sulcus Calcanei Width r = –0.123). These results suggest a high degree of symmetry in calcaneal morphology between the right and left sides.

Talus measurements

The talus measurements are summarized in Tables 4 and 5, and these parameters are shown in Figure 6.

- Trochlear length & width (TL & TW): The left trochlea was slightly longer (21.61 ± 6.85 mm) and wider (23.11 ± 8.46 mm) than the right (20.32 ± ± 8.94 mm, 22.02 ± 9.34 mm), though the differences were not statistically significant (p > 0.05, r = –0.139 to –0.153). These dimensions are crucial for talocrural joint congruency.
- Caput tali height & width (CTH & CTW): Minimal side differences were observed in talar head dimensions, with mean values of approximately 14.4 mm in height and 17.8 mm in width (p > 0.05, r = –0.076 to –0.119).
- Anterior-posterior length (APL): The left talus had a slightly greater APL (65.81 ± 10.34 mm) compared to the right (63.07 ± 9.30 mm), but this difference was not statistically significant (p = 0.309, d = –0.282, 95% CI –9.837 to 4.358). APL plays a key role in dorsiflexion and plantarflexion mechanics.
- Transverse width (TW): The transverse width of the talus was greater on the left (49.14 ± 7.18 mm) than on the right (45.13 ± 5.89 mm), with a moderate effect size (d = –0.631, 95% CI –8.756 to 0.727, p = 0.142). Although the confidence interval included zero, the effect size suggests a potential trend toward lateral asymmetry. This finding, while not statistically significant, may warrant further investigation into subtalar joint biomechanics.
- Sulcus Tali dimensions (SL & SW & SD): No significant differences were found in sulcus length, width, or depth between sides (p > 0.05), indicating uniformity in tendon and ligament pathways. Effect sizes for sulcus tali depth and width were small (d = –0.419 to 0.224, 95% CI –1.036 to 0.271).
- Articular facet areas: The right talus exhibited a slightly larger anterior facet, whereas the left side had larger middle and posterior facets. Statistical analysis, however, showed no significant side preference (p > 0.05, d = –0.322 to –0.306, 95% CI –124.060 to 48.924, –189.259 to 77.479).

Similar to the calcaneus, no statistically significant differences were found between the right and left tali across all measured parameters (p > 0.05). The largest effect size was observed for transverse width (d = –0.631, 95% CI –8.756 to 0.727), indicating a moderate difference between sides, though the confidence interval included zero, confirming a lack of statistical significance. Other parameters exhibited small or negligible effect sizes, with anterior-posterior length (d = –0.282, 95% CI –9.837 to 4.358) and sulcus tali depth (d = –0.419, 95% CI –1.036 to 0.271) showing minor variations. Additionally, rank-biserial correlation values from non-parametric tests confirmed these findings, with anterior articular facet area (r = –0.226) and Middle Articular Facet Area (r = –0.322, 95% CI –124.060 to 48.924) reflecting small but statistically non-significant differences.

In conclusion, no statistically significant anatomical differences were observed between the right and left sides of the calcaneus and talus (p > 0.05), indicating a general pattern of bilateral symmetry. However, Gissane angle (p = 0.063, r = –0.345) and calcaneus maximum width (p = 0.092, r = –0.312) exhibited effect sizes suggesting mild asymmetry, though their confidence intervals included zero, indicating that these differences are not statistically meaningful. Additionally, talus transverse width (p = 0.142, d = –0.631) displayed the largest effect size but did not reach statistical significance, suggesting a potential biomechanical adaptation that warrants further investigation. While some parameters demonstrated small to moderate effect sizes, their confidence intervals included zero, reinforcing the conclusion that these variations are not clinically significant.

Scatter plots for all measured parameters are presented in Figures 9 and 10, demonstrating side-specific variations with overlapping ranges between the right and left sides.

Statistical correlations

- Gissane angle and sulcus calcanei dimensions: A moderate positive correlation was observed

Table 4. Morphometric measurements of the talus between right and left sides.

Parameters	Side	N	Mean	SD	Min	Max	p	r/ Cohen'sd	95% CI
TL	R	16	20.32	8.94	10.04	40.51	0.429	–0.139	(–2.800 to 9.400)
TL	L	16	21.61	6.85	12.90	37.79			
Trochlear width	R	16	22.02	9.34	13.02	44.29	0.386	–0.153	(–1.900 to 11.200)
Trochlear width	L	16	23.11	8.46	15.11	49.87			
CTH	R	16	14.28	5.34	10.35	28.13	0.665	–0.076	(–3.500 to 7.800)
CTH	L	16	14.44	5.00	9.05	27.33			
CTW	R	16	17.63	6.29	12.13	38.11	0.498	–0.119	(–1.700 to 9.900)
CTW	L	16	17.90	4.83	11.01	31.81			
APL	R	16	63.07	9.30	49.40	82.58	0.309	–0.282	(–9.837 to 4.358)
APL	L	16	65.81	10.34	50.41	85.57			
Transverse width	R	16	45.13	5.89	32.98	54.85	0.142	–0.631	(–8.756 to 0.727)
Transverse width	L	16	49.14	7.18	36.88	58.60			
SL	R	16	23.29	4.04	16.30	30.69	1.000	–0.004	(–2.798 to 2.765)
SL	L	16	23.30	3.65	17.14	30.51			
SW	R	16	6.63	1.82	3.30	9.62	0.522	0.224	(–0.842 to 1.553)
SW	L	16	6.27	1.48	3.50	8.70			
Sulcus tali depth	R	16	3.87	0.90	2.35	5.88	0.474	–0.419	(–1.036 to 0.271)
Sulcus tali depth	L	16	4.25	0.91	2.94	5.66			
Anterior articular facet area	R	8	225.33	151.11	83.67	745.27	0.200	–0.226	(–2.800 to 15.300)
	L	11	173.92	65.39	57.35	296.29			
Middle articular facet area	R	11	342.08	231.06	87.21	1103.09	0.309	–0.322	(–124.060 to 48.924)
	L	11	332.77	127.47	48.73	614.37			
Posterior articular facet area	R	16	891.86	183.21	682.29	1288.61	0.309	–0.306	(–189.259 to 77.479)
	L	16	938.89	188.80	604.92	1236.25			

APL — anterior-posterior length; CI — confidence interval; CTH — caput tali height; CTW — Caput tali width; L — left; Max — maximum; Min — minimum; N — sample size; R — right; r — effect size; SD — standard deviation; SL — sulcus tali length; SW — Sulcus tali width; TL — trochlear length.

Table 5. Overall morphometric measurements of the talus.

Parameter	Mean	SD	Min	Max	N
Gissane angle	133.59	7.68	120.89	143.78	29
Böhler angle	37.50	8.53	21.70	52.88	29
Maximum length	91.38	13.47	58.98	110.89	29
Maximum width	52.88	7.44	35.40	62.47	29
Sulcus calcanei length	18.94	6.20	9.63	30.82	29
Sulcus calcanei width	3.50	1.39	1.26	8.16	29
Sulcus calcanei depth	2.87	1.22	0.93	5.32	29
Posterior articular facet area	462.01	313.57	96.20	1100.59	29
Middle articular facet area	250.00	147.69	62.30	579.88	23
Anterior articular facet area	205.51	78.57	24.87	431.90	14

Max — maximum; Min — minimum; SD — standard deviation.

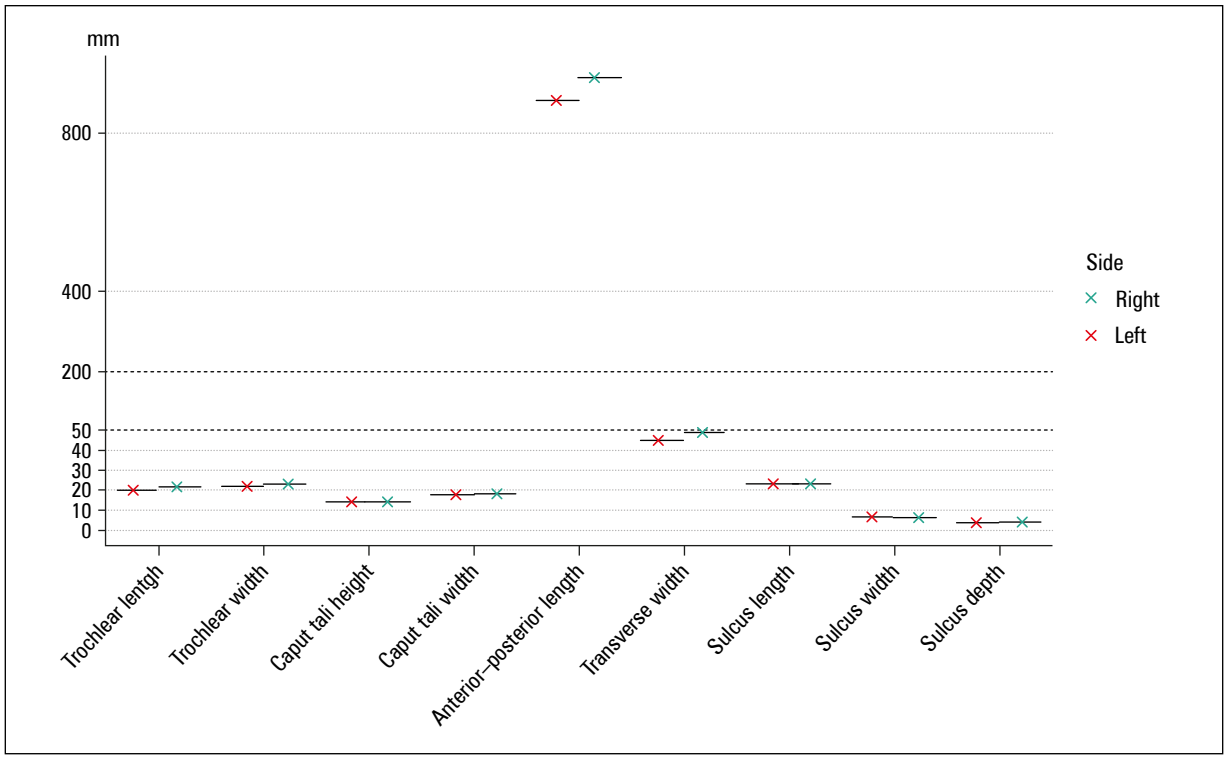


Figure 9. Scatter plot of calcaneus morphometric parameters between right and left sides. This scatter plot compares the values of Gissane angle, Böhler angle, maximum length, maximum width, calcaneal sulcus length, width, depth, and articular facet areas (posterior, middle, anterior) for the calcaneus, showing the overlapping ranges and side-specific trends.

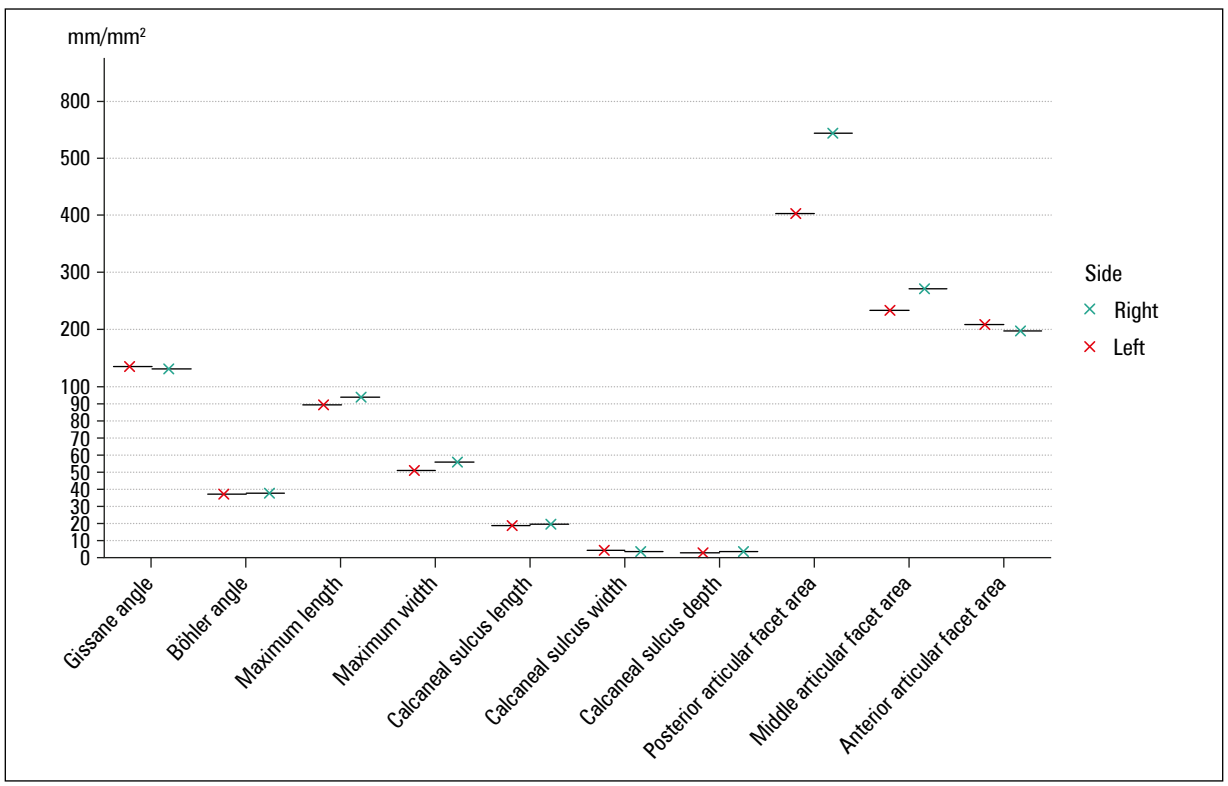


Figure 10. Scatter plot of talus morphometric parameters between right and left sides. This scatter plot highlights the measurements for trochlear length, trochlear width, caput tali height, caput tali width, anterior-posterior length, transverse width, and sulcus dimensions (length, width, depth) for the talus, illustrating overlapping distributions and variations between the sides.

($r = 0.59$, $p < 0.05$), suggesting interdependence in subtalar stability.

- Strong positive correlations were observed between various talus and calcaneus parameters ($p < 0.001$), indicating consistent morphometric relationships.

Facet typing

The classification of talar and calcaneal articular facets is summarized in Tables 6 and 7, and different facet types of the calcaneus and talus are shown in Figures 11–14.

Calcaneus facet types

Right side: The most common facet types were Type B1 and B2, each accounting for 41.2%, followed by Type B3, A2, and A3, each at 5.9%. The dominance of Type B suggests its functional role in lateral weight-bearing and movement stability.

Left side: Type B2 was the most prevalent (50.0%), followed by Type A2 (16.7%), while A1, A3, B1, and B3 each represented 8.3%. The left side exhibited greater morphological diversity, possibly reflecting asymmetrical biomechanical demands.

Talus facet types

Right side: Type B2 was the most frequent (50.0%), followed by Type A1 and B1 (18.8% each) and Type A2 (12.5%). These facet distributions highlight their role in subtalar mobility and joint articulation.

Left side: Type B1 was the most prevalent (37.5%), followed by B2 (31.3%), A1 (18.8%), and A2/A3 (each 6.3%). The differences in facet distributions between sides suggest subtle functional adaptations in subtalar joint mechanics.

Table 6. Distribution of facet types in calcaneus bones between right and left sides.

Side (calcaneus)	Type	N	%
Right	A2	1	5.9
	A3	1	5.9
	B1	7	41.2
	B2	7	41.2
	B3	1	5.9
	Total	17	100.0
Left	A1	1	8.3
	A2	2	16.7
	A3	1	8.3
	B1	1	8.3
	B2	6	50.0
	B3	1	8.3
	Total	12	100.0

Table 7. Distribution of facet types in talus bones between right and left sides.

Side (Talus)	Type	N	%
Right	A1	3	18.8
	A2	2	12.5
	B1	3	18.8
	B2	8	50.0
	Total	16	100.0
Left	A1	3	18.8
	A2	1	6.3
	B1	6	37.5
	B2	5	31.3
	A3	1	6.3
	Total	16	100.0

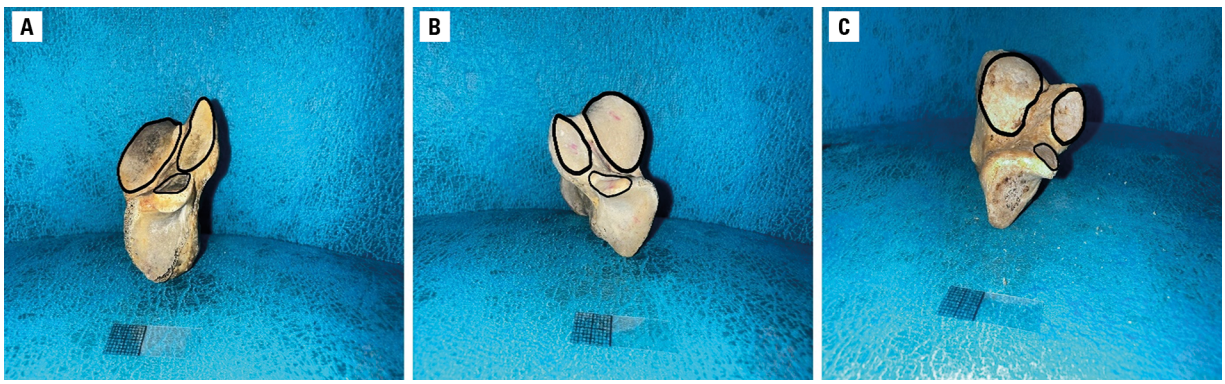


Figure 11. The photographic representation of Type A calcaneus facet configurations, classified based on the distance between the anterior and middle facets; **A.** The distance between the anterior and middle facets is less than 2 mm (Type A1); **B.** The distance between the anterior and middle facets ranges from 2 to 5 mm (Type A2); **C.** The distance between the anterior and middle facets is greater than 5 mm (A3).

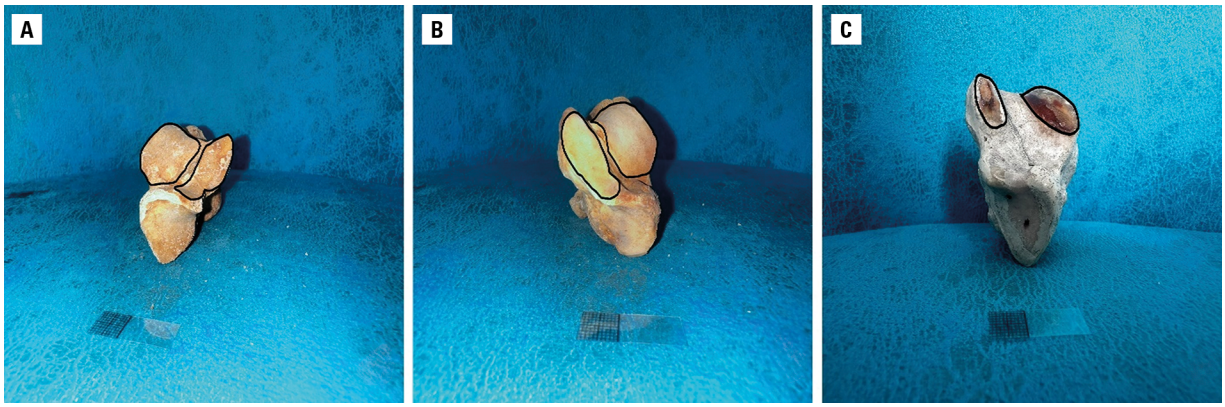


Figure 12. Photographic representation of Type B calcaneus facet configurations, classified according to fusion of the anterior and middle facets and the presence of distinct boundaries; **A.** The anterior and middle facets are fused with smooth transitions and a distinct boundary (Type B1); **B.** The anterior and middle facets are partially fused, with a visible but indistinct boundary (Type B2); **C.** The anterior articular facet is completely absent, with the middle facet present on the superior surface of the sustentaculum tali (Type B3).

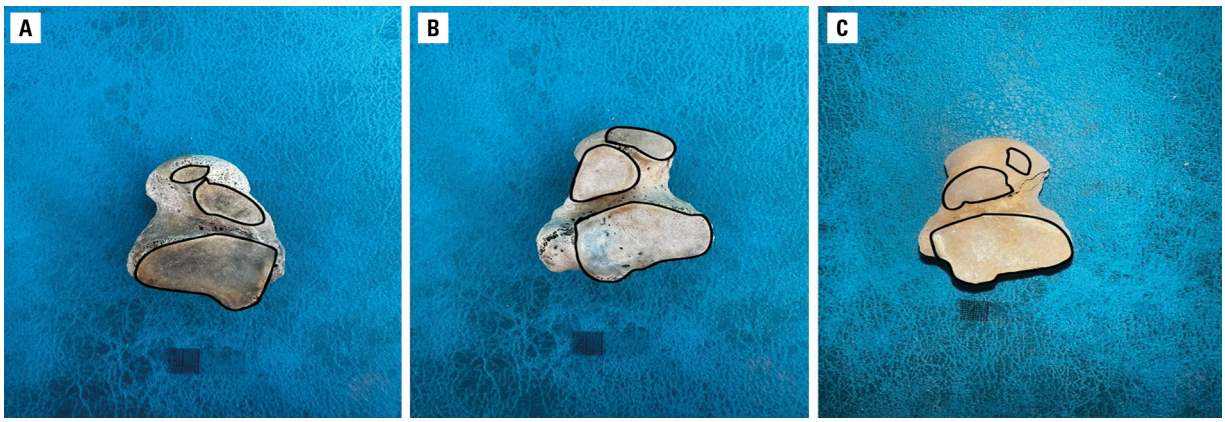


Figure 13. The photographic representation of Type A talus facet configurations, classified based on the distance between the anterior and middle facets; **A.** The distance between the anterior and middle facets is less than 2 mm (Type A1); **B.** The distance between the anterior and middle facets ranges from 2 to 5 mm (Type A2); **C.** The distance between the anterior and middle facets is greater than 5 mm (A3).

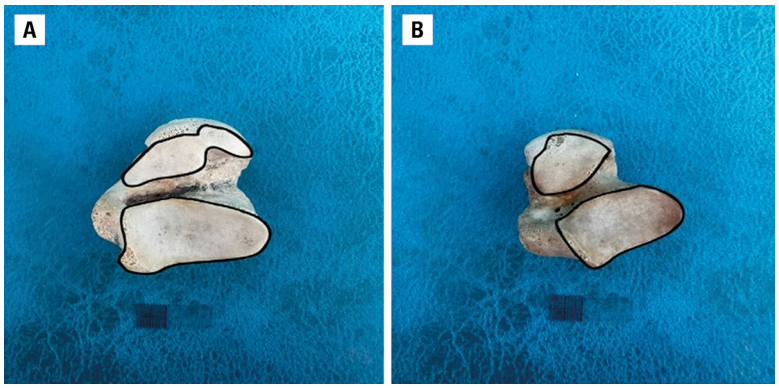


Figure 14. Photographic representation of Type B talus facet configurations, classified according to separation of the anterior and middle facets and the presence of distinct boundaries; **A.** The anterior and middle facets are separated by a narrow gap with a distinct boundary (Type B1); **B.** The anterior and middle facets are separated by a wider gap with a visible but indistinct boundary (Type B2).

DISCUSSION

The analysis of 32 tali and 29 calcanei from the Eastern Anatolian population revealed notable differences in morphometric characteristics and articular facet types compared to other populations reported in the literature. The morphometric measurements and facet classification findings were compared with previous studies and are summarized in Tables 8–12.

Morphometric characteristics of the Eastern Anatolian population

Morphometric analyses are essential in understanding how bone morphology adapts to functional and biomechanical demands. The morphometric measurements of the talus and calcaneus in this study indicate structural variations unique to the Eastern Anatolian population, particularly regarding weight-bearing capacity and postural balance mechanisms.

Although most parameters exhibited high bilateral symmetry and no statistically significant differences, effect size analyses suggested mild asymmetry in certain measurements. Gissane angle and calcaneus maximum width showed moderate effect sizes, while talus transverse width exhibited the largest effect size. However, the confidence intervals for all of these parameters included zero, suggesting that these variations may not represent true anatomical differences but rather subtle biomechanical adaptations.

From a biomechanical perspective, the observed variations may reflect minor adjustments in load transmission and postural control. The slightly wider transverse width of the left talus may suggest subtle modifications in weight-bearing distribution, potentially compensating for asymmetrical locomotor demands. Similarly, the differences in Gissane angle and calcaneal width, although not statistically significant, may indicate lateral column adaptations that could influence subtalar joint kinematics. However, given the small effect sizes and wide confidence intervals, their clinical relevance remains uncertain and requires further investigation through dynamic gait analysis.

Talus morphometry

The talus plays a critical role in joint stability, mobility, and load distribution. The anteroposterior length and transverse width of the talus in this study were significantly larger than those reported in South Indian, Serbian, and previous Anatolian populations [3, 12, 34].

Among the talar parameters, transverse width demonstrated the largest effect size. Although this difference did not reach statistical significance, it suggests a trend toward mild asymmetry in transverse loading patterns, potentially influenced by biomechanical or developmental factors. This finding may have implications for talocrural joint kinematics and requires further investigation with larger sample sizes to determine its clinical relevance.

Table 8. Comparison of Böhler angle (BA) and Gissane angle (GA) across different populations.

Population	N	BA [°]	GA [°]	Reference
American	120	30.0 ± 6.0	–	Chen et al., 1991 [6]
Nigerian	302	32.8 ± 2.8	–	Didia and Dimkpa, 1999 [11]
Ugandan	114	35.1 ± 7.5	–	Igbigbi and Mutesasira, 2002 [19]
Saudi	229	31.2 ± 5.6	116.2 ± 8.5	Khoshhal et al., 2004 [24]
Turkish	308	33.8 ± 4.8	115.0 ± 6.5	Seyahi et al., 2009 [37]
Egyptian	220	30.1 ± 4.1	122.9 ± 6.9	Shoukry et al., 2012 [38]
Korean	42	32.3 ± 5.0	114.4 ± 8.2	Kim et al., 2014 [25]
Indian	184	31.3 ± 4.8	108.7 ± 11.3	Ramachandran and Shetty, 2015 [35]
Nepalese	140	31.3 ± 5.2	108.4 ± 10.5	Rokaya et al., 2016 [36]
Turkish	133	35.3 ± 6.1	111.9 ± 8.5	Yıldız and Çetin, 2019 [44]
Brazilian	800	32.6 ± 6.1	110.6 ± 11.9	Silva Louro et al., 2020 [28]
Turkish	29	37.5 ± 8.6	133.6 ± 7.3	Present study

Table 9. Comparison of calcaneus morphometric measurements across different studies.

	ML (R)	ML (L)	MW (R)	MW (L)	BA(R)	BA(L)	SL (R)	SL (L)	SW (R)	SW (L)
Present study	89.44 ± 15.29	94.13 ± 10.36	50.75 ± 8.10	55.89 ± 5.34	37.28 ± 8.89	37.8 ± 8.35	18.70 ± 6.53	19.29 ± 5.97	3.54 ± 1.58	3.46 ± 1.14
Chavan et al. [40]	88.00 ± 6.37	90.00 ± 5.62	–	–	–	–	–	–	–	–
Dursun et al. [12]	74.87 ± 5.26	76.46 ± 7.36	39.15 ±4.13	39.57 ±3.16	30.18 ±7.45	27.0 ± 5.61	23.00 ± 4.11	21.62 ± 4.56	6.05 ± 1.90	5.20 ± 1.41
Boyan et al. [3]	75.69 ± 6.76	76.07 ± 5.44	45.84 ± 4.21	43.92 ± 3.97	–	–	32.42 ± 3.23	31.85 ± 2.76	5.53 ± 1.00	6.43 ± 1.19
Ari & Kafa [1]	75.00 ± 7.10	74.30 ± 8.40	44.00 ± 5.30	43.50 ± 4.30	–	–	–	–	4.50 ± 0.24	3.80 ± 0.36
Prasad & Rajasekhar [34]	75.30 ± 6.16	75.24 ± 5.10	43.40 ± 3.59	39.73 ± 5.10	–	–	11.92 ± 1.34	10.61 ± 2.67	5.70 ± 1.58	5.62 ± 1.93
Uygur et al. [41]	77.50 ± 5.70	77.90 ± 5.60	48.10 ± 4.00	46.90 ± 4.40	30.09 ± 5.00	30.8 ± 4.90	30.00 ± 3.00	30.80 ± 3.20	6.60 ± 1.00	7.00 ± 1.30
Vučinić et al. [43]	77.30 ± 5.80 (M)	72.50 ± 4.60 (F)	43.20 ± 3.90 (M)	39.60 ± 3.50 (F)	29.50 ± 6.20 (M)	28.1± 5.80 (F)	–	–	15.60 ± 2.30 (M)	14.20 ± 2.00 (F)
Jung et al. [21]	–								4.8–5.4 (Type-specific)	
Otağ et al. [33]	76.21 ± 5.68	76.14 ± 5.53	42.97 ± 3.75	43.51 ± 3.34	29.97 ± 5.22	28.5± 5.00	–	–	4.96 ± 1.48	5.28 ± 1.16
Güler et al. [17]	73.86 ± 5.16	75.26 ± 4.16	26.76 ± 3.61	25.55 ± 1.85	–	–	–	–	–	–
Ergür et al. [13]	74.70 ± 5.80	32.80 ± 3.80	–	–	–	–	–	–	–	–
Garg et al. [16]	71.02 ± 5.06	70.61 ± 4.52	41.48 ± 2.61	40.1 ± 3.36	–	–	45.91 ± 3.17	46.52 ± 3.44	5.34 ± 1.30	6.08 ± 1.23
Dhakal et al. [10]	70.22 ± 7.10	70.47 ± 8.79	38.36 ± 4.17	38.77 ± 3.87	34.92 ± 8.09	35.4 ± 7.30	–	–	–	–
Singh et al. [39]	78.20 ± 5.60		46.30 ± 4.20		33.40 ± 3.80		–		5.90 ± 1.50	
Jyotsna&Mamidi [31]	76.01 ± 5.74		45.94 ± 4.35		32.81 ± 3.78		–		5.63 ± 1.01	

BA — Böhler angle; F — female; L — left; M — male; ML — maximum length; MW — maximum width; R — right; SL — calcaneal sulcus length; SW — calcaneal sulcus width.

Table 10. Comparison of talus morphometric measurements across different studies.

	APL	TW	SL	SW	SD	TL
Present Study	64.44 ± 9.77	47.14 ± 6.77	23.29 ± 3.79	6.45 ± 1.64	4.06 ± 0.91	20.97 ± 7.86
Dursun et al. [12]	55.34 ± 5.49	41.22 ± 3.84	21.95 ± 3.20	6.09 ± 1.51	–	–
Boyan et al. [3]	53.05 ± 4.38	39.33 ± 3.66	21.06 ± 3.66	6.08 ± 2.05	5.66 ± 1.52	–
Ari & Kafa [1]	57.20 ± 4.00	49.10 ± 3.30	21.00 ± 4.50	5.80 ± 1.40	–	31.50 ± 3.20
Prasad & Rajasekhar [34]	50.51 ± 3.90	36.29 ± 2.94	12.24 ± 2.87	5.65 ± 1.30	3.97 ± 1.02	–
Jung et al. [21]	–	–	–	–	–	42–54 (Type-specific)
Ilgaz & Ülkir [20]	55.08 ± 4.12	41.71 ± 3.44	20.19 ± 2.43	5.93 ± 1.15	6.75 ± 1.29	33.58 ± 2.84
Garg et al. [16]	51.14 ± 4.50 (R) 50.89 ± 3.81 (L)	37.90 ± 2.90 (R) 37.84 ± 3.27 (L)	18.21 ± 2.60 (R) 18.70 ± 2.80 (L)	7.13 ± 1.78 (R) 6.75 ± 1.50 (L)	5.44 ± 0.53 (R) 5.05 ± 0.33 (L)	–

APL — anterior–posterior length; SD — sulcus tali depth; SL — sulcus tali length; SW — sulcus tali width; TL — trochlear length; TW — transverse width.

Table 11. Comparison of calcaneus facet types across different studies.

	A1 [%]	A2 [%]	A3 [%]	A4 [%]	B1 [%]	B2 [%]	B3 [%]	C [%]
Present Study	0.0 (R) 8.3 (L)	5.9 (R) 16.7 (L)	5.9 (R) 8.3 (L)	–	41.2 (R) 8.3 (L)	41.2 (R) 50.0 (L)	5.9 (R) 8.3 (L)	–
Jyotsna & Mamidi [31]	2.04	7.14	8.06	2.04	27.55	53.06	–	–
Dursun et al. [12]	5.5	16.6	5.5	–	27.7	44.4	–	–
Boyan et al. [3]	7.4	14.8	11.1	3.7	22.2	40.8	–	–
Prasad & Rajasekhar [34]	–	–	–	–	58.7	96.8	–	–
Güler et al. [17]	43.3	33.3	–	–	10.0	26.7	–	–
Garg et al. [16]	–	–	–		40.0 (R) 33.3 (L)	43.3 (R) 46.7 (L)	–	3.3 (R) 0.0 (L)
Singh et al. [39]	4.7	4.7	5.8	9.3	23.3	51.2	–	1.2
Taqdees et al. [14]	46.0	–	27.3	–	15.3	5.3	–	2.0
Dhakal et al. [10]	56.3 57.5 (R) 42.5 (L)	–	–	1.4 0.0 (R) 1.4 (L)	–	–	0.0 0 (R) 0 (L)	42.2 38.3 (R) 61.6 (L)

L — left; R — right.

One possible explanation for this increase in talar size is the geographical and environmental challenges faced by the Eastern Anatolian population. Navigating rugged and mountainous terrain may have necessitated a broader load-bearing surface, enhancing joint stability and shock absorption [45]. Additionally, the larger subtalar joint surface in this population likely improves force dissipation and postural balance.

The sulcus tali was found to be narrower and shallower compared to previous studies [16, 20]. This variation may result in increased pressure on the flexor hallucis longus tendon, potentially restricting tendon mobility and increasing the risk of impingement syndromes. However, a narrower sulcus may also enhance tendon stabilization, optimizing muscle-tendon interaction and reducing excessive flexion movements [22].

Furthermore, the trochlear width and length were larger in this study than those recorded in other populations [3, 12, 34]. A broader trochlear surface may facilitate more efficient load distribution, thereby reducing stress on the subtalar joint [33, 40]. From a clinical perspective, these findings highlight the

Table 12. Comparison of talus facet types across different studies.

	A1 [%]	A2 [%]	A3 [%]	B1 [%]	B2 [%]	B3 [%]	C [%]
Present study	18.8 (R) 18.8 (L)	12.5 (R) 6.3 (L)	0.0 (R) 6.3 (L)	18.8 (R) 37.5 (L)	50.0 (R) 31.3 (L)	–	–
Jyotsna & Mamidi [31]	–	–	–	–	–	–	–
Dursun et al. [12]	–	8.6	–	17.3	73.9	–	–
Boyan et al. [3]	–	–	–	–	–	–	–
Ari & Kafa [1]	–	–	–	–	–	–	–
Prasad & Rajasekhar [34]	–	–	–	58.7	96.8	–	–
Jung et al. [21]	–	11.0	–	46.6	–	–	42.4
Ilgaz & Ülkir [20]	1.1	3.4	–	65.5	29.9	–	–
Garg et al. [16]	–	–	–	46.1 (R) 45.8 (L)	26.9 (R) 45.8 (L)	–	19.2 (R) 8.3 (L)

L — left; R — right.

need for careful preoperative assessment in ankle arthroscopy and total ankle replacement procedures to ensure optimal joint congruency and implant selection.

Although not statistically significant, asymmetrical dimensions of the medial and lateral articular surfaces of the talus suggest unequal biomechanical load distribution. This asymmetry may contribute to postural adaptations and weight transmission during gait, underscoring its relevance in orthopedic surgical planning and rehabilitation strategies [2, 9].

Calcaneus morphometry

The calcaneus is the primary weight-bearing bone of the foot, playing a crucial role in mobility, impact absorption, and stability. In this study, the anteroposterior length and transverse width of the calcaneus were greater than those reported in South Indian, Anatolian, and Serbian populations [12, 32].

Böhler's and Gissane's angles, which are essential for shock absorption and subtalar joint stability, were higher than those reported in previous studies [33, 37]. A higher Böhler's angle is generally associated with greater load-bearing capacity and enhanced resistance to fractures, while an increased Gissane's angle may contribute to improved subtalar joint balance and force distribution. However, an excessively high Gissane's angle could also elevate the risk of subtalar joint osteoarthritis [18].

Effect size analyses revealed that, although most calcaneal parameters showed negligible differences between sides, Gissane angle and maximum width exhibited moderate effect sizes. These findings suggest possible asymmetry in lateral calcaneal morphology, which may influence subtalar joint biomechanics. While these differences were not statistically significant, they may still have clinical relevance in the evaluation of joint stability, force distribution, and osteoarthritic risk.

Although some parameters, such as maximum width and sulcus calcanei depth, exhibited small but non-significant differences, the sulcus calcanei was narrower and shallower than in previous studies [29, 43].

The environmental and biomechanical demands of the Eastern Anatolian region, characterized by rugged terrain and variable load-bearing conditions, may have influenced adaptive morphological changes in the calcaneus. A longer and wider calcaneus likely enhances stability on uneven surfaces, facilitating more efficient weight transfer and impact absorption. This adaptation may be particularly advantageous for populations that historically relied on prolonged walking and climbing over irregular landscapes. Conversely, the narrower and shallower sulcus calcanei observed in this population may serve to optimize tendon stabilization and energy efficiency during gait. However, this configuration could also increase the risk of tendon impingement syndromes, particularly affecting the flexor hallucis longus and tibialis posterior tendons, which are critical for foot propulsion and arch support [37, 40]. While these structural differences do not necessarily indicate pathological outcomes,

they highlight population-specific anatomical adaptations that may influence both clinical assessment and orthopedic treatment strategies [16, 22].

From a clinical and surgical perspective, calcaneal morphometric characteristics have significant implications for subtalar joint biomechanics and orthopedic procedures. The larger Böhler's angle observed in this study suggests a potentially lower risk of post-traumatic calcaneal deformity, which may impact fracture management strategies and post-surgical outcomes.

Overall, the morphometric adaptations observed in the Eastern Anatolian population are likely driven by a combination of genetic, environmental, and biomechanical factors. Understanding these structural variations provides valuable insights for clinical applications, particularly in personalized surgical planning and rehabilitation protocols.

Articular facet typing and functional implications

Articular facet classification plays a fundamental role in understanding subtalar joint biomechanics, as different facet configurations influence joint mobility, weight distribution, and stability. In this study, we identified a predominance of Type B facets, particularly the B2 and B3 subtypes, which aligns with findings from previous studies on Anatolian populations but demonstrates notable differences in distribution and prevalence compared with other geographic populations [3, 12, 16].

Among the identified facet types, Type B3 facets were found to be more frequent in this population than previously reported in the literature, suggesting a potentially distinct morphological adaptation in the Eastern Anatolian population. This configuration, characterized by the absence of an anterior facet, may influence subtalar joint function by limiting excessive inversion and eversion movements, potentially reducing the risk of instability-related injuries. However, this reduction in mobility could also lead to increased joint stiffness and altered force distribution, predisposing individuals to degenerative conditions such as subtalar joint arthritis, particularly in those with high physical activity levels. From a clinical perspective, the predominance of Type B3 facets should be considered in surgical interventions like subtalar arthrodesis and ligament reconstruction, as joint congruency and fusion techniques may require modifications based on facet morphology. Additionally, forensic anthropologists may use facet type distributions as distinguishing features in population-specific skeletal identification, highlighting the anatomical and functional significance of these morphological variations [34].

The presence of Type A facets, though less frequent, is consistent with previous reports and provides insight into the functional diversity of subtalar articulation. Type A facets, associated with greater subtalar mobility, were observed to be more common on the left side in our study. This asymmetry may indicate biomechanical adaptations that favor medial stability while preserving lateral flexibility, potentially playing a role in weight-bearing efficiency during gait and postural adjustments [20, 22].

Additionally, side-specific variations in facet distribution provide further insights into the biomechanical demands acting on the subtalar joint. The predominance of Type B facets on the right side suggests a lateral stability adaptation, which could be associated with a dominant weight-bearing function in right-sided locomotion patterns. This hypothesis is supported by studies indicating that variations in subtalar facet morphology are influenced by repetitive mechanical loading and postural alignment [18, 45].

The clinical significance of these facet configurations is particularly relevant in the context of orthopedic and reconstructive surgical procedures. Understanding the distribution of facet types is crucial for preoperative planning in subtalar joint fusion (arthrodesis), subtalar prosthetic implant placement, and ligament reconstruction procedures. The predominance of Type B3 facets may present challenges in achieving optimal joint congruency during surgical interventions, while the variability in facet orientations could influence rehabilitation strategies and postoperative functional outcomes [23, 40].

Overall, these findings reinforce the importance of population-specific anatomical studies in clinical and biomechanical research, emphasizing the need for tailored surgical approaches based on facet morphology. Future studies should further investigate the dynamic impact of facet variations on joint kinematics and their potential role in injury susceptibility and degenerative joint disorders [2, 9].

Adaptations to environmental, genetic, and biomechanical factors

The morphological adaptations observed in the talus and calcaneus of the Eastern Anatolian population

reflect a complex interplay between genetic, environmental, and biomechanical influences. The region's rugged terrain, high altitudes, and historical lifestyle factors, including increased physical activity and weight-bearing demands, have likely contributed to distinct skeletal characteristics that optimize locomotion efficiency and joint stability. Additionally, genetic predispositions may have played a role in shaping the talocalcaneal architecture, as population-specific variations in bone morphology can arise from both heritable traits and long-term mechanical loading patterns [2, 26].

Despite the overall symmetry observed in both bones, subtle morphometric differences with small to moderate effect sizes suggest possible biomechanical adaptations rather than true anatomical asymmetry. The greater transverse width of the talus on the left side may indicate a functional adjustment related to weight-bearing mechanics or postural stability, while variations in Gissane angle and maximum width could reflect minor adaptations in lateral column loading. However, given that these differences did not reach statistical significance, they are unlikely to have a major clinical impact. These features are advantageous for individuals who frequently traverse uneven terrain, as they help mitigate the impact forces exerted on the subtalar and ankle joints. The prominence of these structural adaptations aligns with findings from populations that engage in high levels of walking and climbing, reinforcing the hypothesis that habitual physical activity influences lower limb skeletal morphology [2, 8].

In contrast, the narrower sulcus tali and sulcus calcanei suggest evolutionary constraints that enhance tendon stabilization at the expense of reduced tendon mobility. While this configuration minimizes excessive tendon displacement and enhances energy efficiency during gait, it may also predispose individuals to tendon entrapment syndromes, impingement, and chronic pain conditions such as flexor hallucis longus tendonitis [12, 34]. These findings emphasize the importance of understanding population-specific variations in tendon and ligament function, as they have direct implications for diagnosing and managing musculoskeletal pathologies.

Another key observation is the asymmetric distribution of facet types between the right and left feet. The predominance of Type B facets on the right side suggests a lateral stability adaptation that enhances balance and weight-bearing efficiency, whereas the increased prevalence of Type A facets on the left side may reflect a functional adaptation for medial load distribution. These variations highlight the role of biomechanical forces in shaping skeletal morphology, supporting previous research that links articular facet variations to gait mechanics and postural adaptations [22, 26].

The presence of Type B3 facets, which lack an anterior facet, may indicate a reduction in subtalar joint mobility. While this configuration provides increased joint stability, it also limits flexibility, which could be a compensatory adaptation to high-impact locomotor activities. This aligns with previous studies that suggest subtalar joint morphology plays a crucial role in determining overall foot function and stability [18, 45].

Overall, the findings of this study emphasize the impact of environmental, genetic, and biomechanical factors on foot morphology. The historical reliance of the Eastern Anatolian population on rugged terrain and physically demanding activities may have played a role in shaping the talocalcaneal architecture. Future research incorporating genetic analyses and comparative biomechanical studies across diverse populations could provide deeper insights into the interplay between evolutionary adaptations and functional demands. These adaptations provide crucial insights into evolutionary trends in human locomotion and highlight the importance of considering population-specific anatomical variations in clinical and orthopedic evaluations. Understanding these morphological traits can improve rehabilitation strategies, prosthetic design, and surgical decision-making for individuals with subtalar joint abnormalities [16, 21].

Clinical and surgical relevance

The clinical and surgical relevance of the findings of this study lies in improving orthopedic, rehabilitative, and surgical approaches to foot and ankle conditions. The morphometric variations observed in the talus and calcaneus of the Eastern Anatolian population have direct implications for diagnosing musculoskeletal disorders, planning reconstructive procedures, and optimizing prosthetic design.

Implications for orthopedic and trauma surgery

The variations in talar and calcaneal morphology influence the biomechanics of weight-bearing and

gait. The predominance of Type B facets, particularly Type B2 and B3, suggests altered subtalar joint kinematics, which may necessitate modifications in surgical techniques for treating subtalar instability, arthrodesis, and total ankle replacements [12, 20]. The increased dimensions of the talus and calcaneus may affect fracture patterns and the selection of orthopedic implants. The higher Böhler's and Gissane's angles observed indicate potential variations in load transmission and fracture healing dynamics, emphasizing the importance of individualized surgical planning [37, 40].

While statistical analyses confirmed that morphometric variations between the right and left sides were not statistically significant, effect size analyses indicated small to moderate asymmetries in certain parameters. These variations suggest that although the bones are largely symmetric, minor structural adaptations may still exist. From a surgical perspective, these findings reinforce the applicability of generalized morphometric reference values, while also highlighting the need to consider individual variations, particularly in reconstructive procedures involving the subtalar joint and ankle complex.

Considering the observed variations in facet morphology and minor morphometric asymmetries, surgical approaches should be tailored to individual anatomical features rather than assuming complete bilateral symmetry. The predominance of Type B3 facets may necessitate specific considerations in procedures such as subtalar arthrodesis, as this configuration could influence postoperative mobility and stability. Additionally, variations in subtalar joint morphology may be relevant for implant design in total ankle arthroplasty, requiring further biomechanical validation to optimize functional outcomes. Clinicians should integrate population-specific morphometric reference data into surgical planning, particularly in cases involving subtalar instability or degenerative joint disease.

Impact on foot and ankle pathologies

The narrower sulcus tali and sulcus calcanei suggest a predisposition to tendon entrapment syndromes, including flexor hallucis longus tendonitis and posterior tibial tendon dysfunction [32, 34]. These anatomical constraints can alter tendon gliding and contribute to chronic foot pain and restricted mobility. Furthermore, the identified asymmetry in facet distribution may correlate with an increased risk of unilateral degenerative changes in the subtalar joint, necessitating early clinical intervention [3, 40].

Surgical considerations in joint reconstruction

Surgeons performing ankle arthrodesis or subtalar fusion must account for facet morphology to optimize joint congruency and stability [22, 41]. The high prevalence of Type B3 facets, characterized by the absence of an anterior facet, may complicate surgical fixation techniques and influence post-operative outcomes. In addition, morphometric variations should be integrated into preoperative imaging analysis to enhance precision in osteotomy planning and implant selection [21]. These findings highlight the importance of incorporating biomechanical validation in surgical decision-making to optimize functional outcomes.

Forensic and anthropological applications

The unique morphometric characteristics of the talus and calcaneus in this population provide valuable data for forensic identification and population-specific skeletal analysis [2, 8]. The observed anatomical adaptations, likely influenced by environmental and genetic factors, contribute to a broader understanding of human skeletal diversity and its implications in forensic casework.

This study's findings align with certain previous studies in the literature; however, notable differences in morphometric measurements and subtalar joint facet distributions were observed [3, 12]. Several factors contribute to these discrepancies. First, methodological variations are a major factor. Many previous studies have relied on radiographic analysis or manual caliper-based measurements, which can introduce observer bias and measurement inconsistencies [2, 12, 18, 27, 29]. In contrast, our study utilized three-dimensional (3D) modeling and digital measurement techniques, allowing for a more detailed and reproducible examination of bony structures. This methodological advancement enhances measurement precision and comparability with clinical imaging applications, potentially identifying subtle morphological differences that prior methods may have overlooked. Second, population-specific differences must be considered. Previous studies have predominantly examined broadly defined populations, such as South Asian, Balkan, and Western European groups,

but detailed regional adaptation studies remain scarce [10, 11, 14, 16, 19, 24, 26–29, 35, 38, 43, 45]. Our study fills this gap by focusing on a distinct Eastern Anatolian population, which may exhibit unique genetic and environmental influences that contribute to talocalcaneal morphology variations. Third, biomechanical and environmental adaptations likely play a role. The historical adaptation of individuals in this region to rugged terrains, long-distance walking, and distinct footwear habits may have influenced subtalar joint facet distribution and bone adaptation, contributing to differences observed in our study. While previous studies have provided descriptive morphometric data, many lacked in-depth statistical assessments of biological relevance, often reporting variations without considering effect sizes, confidence intervals, or other critical parameters [10, 12, 16, 34, 39]. Our study integrates a more refined statistical framework, allowing for a more precise interpretation of morphometric differences and their functional implications. This not only strengthens the reliability of our findings but also enhances their applicability in clinical and forensic contexts. Moreover, previous research has rarely discussed the functional and surgical relevance of these morphometric differences [1, 39]. This study builds upon and refines this knowledge by linking morphometric variations to subtalar joint function, weight-bearing efficiency, and orthopedic surgical considerations. Additionally, while skeletal morphometry is widely used in forensic anthropology, most existing datasets lack region-specific reference values. This study contributes a new dataset specific to the Eastern Anatolian population, improving forensic identification methodologies by capturing unique regional skeletal traits. In summary, while previous studies have laid the foundation for understanding talocalcaneal morphology, our research advances this field by incorporating 3D measurement techniques, a refined statistical approach, and a population-specific focus, addressing existing gaps and offering new insights into subtalar biomechanics in both normal and pathological conditions.

Study limitations

While this study provides valuable insights into the morphological characteristics of the talus and calcaneus in the Eastern Anatolian population, certain limitations must be acknowledged. First, the sample size, although sufficient to identify significant morphological patterns, remains relatively limited for broader generalization. This limitation may affect the ability to detect rarer phenotypes and perform more detailed interpopulation comparisons. The sample size also restricts the ability to evaluate variations influenced by demographic factors such as age and sex, which are crucial in determining bone shape and structure. Sexual dimorphism and age-related changes can influence joint congruency, facet morphology, and weight-bearing adaptations. Future studies should incorporate larger datasets to enhance statistical power and provide more comprehensive population-level insights.

Additionally, the absence of demographic data, such as age and sex, limits the ability to evaluate inter-individual and sex-related variations in talus and calcaneus morphology. These variables play a crucial role in determining bone shape and structure, as sexual dimorphism and age-related changes can influence joint congruency, facet morphology, and weight-bearing adaptations [12, 16]. Future studies should prioritize datasets with detailed demographic information to analyze these variations systematically.

Strengths of the study

Despite these limitations, this study possesses several strengths that enhance its scientific and clinical value. The use of three-dimensional (3D) model reconstruction allowed for highly detailed morphometric assessments, providing a more precise representation of anatomical variations compared to traditional two-dimensional imaging methods. The comprehensive analysis of both morphometric parameters and facet classifications offers an in-depth understanding of talus and calcaneus morphology in a previously underrepresented population. Additionally, comparisons with multiple populations worldwide enable a broader perspective on interpopulation differences, contributing to the field of forensic anthropology, orthopedic surgery, and anatomical research.

Directions for future research

Future research should further investigate the relationship between facet morphology and subtalar joint biomechanics, particularly in relation to joint stability and mobility. The predominance of Type B3 facets in this population raises questions about its functional significance, particularly in relation to subtalar

joint stability and mobility. Future research should incorporate dynamic gait analysis and biomechanical modeling to assess how these morphological differences influence movement patterns, postural stability, and susceptibility to orthopedic conditions such as osteoarthritis.

Genetic studies examining the heritability of these traits may contribute to a deeper understanding of population-specific anatomical variations. Cross-population comparative studies, particularly with groups exposed to distinct environmental pressures, would help determine whether these adaptations are primarily genetic or the result of long-term biomechanical demands.

Lastly, the clinical implications of these findings warrant further exploration in orthopedic and forensic applications. The identification of morphometric variations in subtalar structures can aid in forensic reconstructions, surgical planning, and prosthetic design, particularly in regions where population-specific anatomical data are scarce. Future research should also investigate the long-term effects of these structural adaptations on joint health, injury risk, and rehabilitation outcomes.

By addressing these limitations and expanding the scope of investigation, future research can provide a more nuanced understanding of subtalar joint morphology and its implications for biomechanics, evolution, and clinical practice.

CONCLUSIONS

Incorporating these findings into clinical and biomechanical applications enhances the understanding of subtalar joint morphology, shedding light on its role in maintaining joint stability, facilitating mobility, and supporting overall foot function. Additionally, these findings highlight the necessity of considering population-specific anatomical differences in orthopedic practice, forensic anthropology, and biomechanical modeling. Integrating these data into clinical decision-making and surgical strategies will improve patient outcomes and enhance the precision of musculoskeletal interventions. Future research should focus on the genetic, environmental, and functional factors contributing to these variations, further advancing the integration of anatomical data into clinical and biomechanical contexts.

ARTICLE INFORMATION AND DECLARATIONS

Data availability statement

The datasets used in this report are available from the corresponding author upon reasonable request.

Ethics statement

This study was approved by the Atatürk University Non-Interventional Clinical Research Ethics Committee.

Author contributions

Project development: ABK, YA, BY, MS. Data collection and analysis: ABK. Manuscript writing and editing: ABK. Editing: YA, BY, MS.

Funding

The authors declare they have not received any financial support.

Conflict of interest

The authors declare that they have no conflict of interest.

Supplementary material

None.

REFERENCES

1. Ari I, Kafa IM. Bone length estimation and population-specific features of calcaneus and talus bones of the late Byzantine Era. Coll Antropol. 2009; 33(2): 613–618, indexed in Pubmed: 19662787.
2. Bidmos M. Metrical and non-metrical assessment of population affinity from the calcaneus. Forensic Sci Int. 2006; 159(1): 6–13, doi: 10.1016/j.forsciint.2005.06.005, indexed in Pubmed: 16051455.
3. Boyan N, Ozsahin E, Kizilkanat E, et al. Morphometric measurement and types of articular facets on the talus and calcaneus in an Anatolian population. Int J Morphol. 2016; 34(4): 1378–1385, doi: 10.4067/s0717-95022016000400033.
4. Bunning PS, Barnett CH. A comparison of adult and foetal talocalcaneal articulations. J Anat. 1965; 99(Pt 1): 71–76, indexed in Pubmed: 14245347.
5. Forriol Campos F, Gomez Pellico L. Talar articular facets (facies articulares talares) in human calcanei. Acta Anat (Basel). 1989; 134(2): 124–127, doi: 10.1159/000146675, indexed in Pubmed: 2718725.
6. Chen MY, Bohrer SP, Kelley TF. Boehler's angle: a reappraisal. Ann Emerg Med. 1991; 20(2): 122–124, doi: 10.1016/s0196-0644(05)81206-5, indexed in Pubmed: 1996790.

7. Chen Z, Wang Y, Li X, et al. An automatic measurement system of distal femur morphological parameters using 3D slicer software. Bone. 2022; 156: 116300, doi: 10.1016/j.bone.2021.116300, indexed in Pubmed: 34958998.
8. Cockerill SJ, Arnay-de-la-Rosa M, González-Reimers E. An atlas of anatomical variants of the human calcaneus. J Morphol. 2024; 285(5): e21706, doi: 10.1002/jmor.21706, indexed in Pubmed: 38704702.
9. Cowin SC. The mechanical and stress adaptive properties of bone. Ann Biomed Eng. 1983; 11(3-4): 263–295, doi: 10.1007/BF02363288, indexed in Pubmed: 6670786.
10. Dhakal A, Adhikari P, Khan G, et al. Patterns of superior articular facet and morphometric study of Nepalese dry Calcanei. Sanamed. 2018; 13(2): 17–22, doi: 10.24125/sanamed.v13i1.217.
11. Didia BC, Dimkpa JN. The calcaneal angle in Nigerians. Relationship to sex, age, and side of the body. J Am Podiatr Med Assoc. 1999; 89(9): 472–474, doi: 10.7547/87507315-89-9-472, indexed in Pubmed: 10507216.
12. DURSUN A, YILMAZ V, KASTAMONİ Y, et al. Anadolu Popülasyonunda Talus ile Calcaneus'un Morfometrik Özellikleri ve Ortak Eklem Yüzlerinin Tiplendirilmesi. Süleyman Demirel Üniversitesi Sağlık Bilim Derg. 2021; 12(3): 351–363, doi: 10.22312/sdusbed.961431.
13. ERGÜR İ, KOŞAY C, ZEYBEK G, et al. Morphologic and morphometric variations of calcaneus and their importance in surgical procedures. Turkiye Klin J Med Sci. 2011; 31(1): 15–21, doi: 10.5336/medsci.2009-14722.
14. Fatima T. Study of pattern of the talar articular facets in 150 dried adult human calcanei of North Karnataka population. Int J Anat Res. 2021; 9(3.1): 8040–8044, doi: 10.16965/ijar.2021.141.
15. Fedorov A, Beichel R, Kalpathy-Cramer J, et al. 3D Slicer as an image computing platform for the Quantitative Imaging Network. Magn Reson Imaging. 2012; 30(9): 1323–1341, doi: 10.1016/j.mri.2012.05.001, indexed in Pubmed: 22770690.
16. Garg S, Verma U, Suri A, et al. Morphometric analysis and types of articular facets on human dry tali and calcanei of north Indian origin. Biomedicine. 2022; 42(1): 28–32, doi: 10.51248/.v42i1.959.
17. Güler H, Uçar S, Ekinci HG, et al. Calcaneus'un antropometrik Ölçümünün Klinik Önemi. Sağlık Bilimleri Dergisi. 2022; 31(1): 45–50, doi: 10.34108/eujhs.858800.
18. Gültekin A, Acar E, Uğur L, et al. The importance of Böhler's angle in calcaneus geometry: a finite element model study. Jt Dis Relat Surg. 2021; 32(2): 420–427, doi: 10.52312/jdrs.2021.81251, indexed in Pubmed: 34145820.
19. Igbigbi PS, Msamati BC. The calcaneal angle in indigenous Malawian subjects. The Foot. 2002; 12(1): 27–31, doi: 10.1054/foot.2001.0715.
20. ILGAZ H, ÜLKİR M. Talus kemiğinin bazı morfolojik ve morfometrik özelliklerinin değerlendirilmesi. Kocaeli Üniversitesi Sağlık Bilim Derg. 2022; 8(2): 134–138, doi: 10.30934/kusbed.1020790.
21. Jung MH, Choi BY, Lee JiY, et al. Types of subtalar joint facets. Surg Radiol Anat. 2015; 37(6): 629–638, doi: 10.1007/s00276-015-1472-1, indexed in Pubmed: 25822134.
22. Kanamoto S, Ogihara N, Nakatsukasa M. Three-dimensional orientations of talar articular surfaces in humans and great apes. Primates. 2011; 52(1): 61–68, doi: 10.1007/s10329-010-0219-1, indexed in Pubmed: 20844922.
23. Karakas AB, Govsa F, Ozer MA, et al. 3D brain imaging in vascular segmentation of cerebral venous sinuses. J Digit Imaging. 2019; 32(2): 314–321, doi: 10.1007/s10278-018-0125-4, indexed in Pubmed: 30242780.
24. Khoshhal KI, Ibrahim AF, Al-Nakshabandi NA, et al. Böhler's and Gissane's angles of the calcaneus in the Saudi population. Saudi Med J. 2004; 25(12): 1967–1970, indexed in Pubmed: 15711677.
25. Kim JH, Gwak HC, Kim JG, et al. Measurement of normal calcaneus in korean cadavers: a preliminary report. J Korean Foot Ankle Soc. 2014; 18(1): 14, doi: 10.14193/jkfas.2014.18.1.14.
26. Koh D, Tan B, Mehta K, et al. Morphometric analysis of the calcaneus in a Southeast Asian population. Cureus. 2024; 16(4): e58899, doi: 10.7759/cureus.58899, indexed in Pubmed: 38800141.
27. Kori D, Prasad G, Rani A, et al. Study of variations in talar articular facets of human calcanei and their association with calcaneal spurs in north indian population. Int J Anat Res. 2016; 4(3.2): 2710–2716, doi: 10.16965/ijar.2016.313.
28. da Silva Louro EC, Faleiro T, Pereira T, et al. Radiographic study of Böhler and Gissane angles in the Brazilian population. J Foot Ankle. 2020; 14(1): 57–61, doi: 10.30795/jfootankle.2020.v14.1167.
29. Madhavi C, Madhuri V, George VM, et al. South Indian calcaneal talar facet configurations and osteoarthritic changes. Clin Anat. 2008; 21(6): 581–586, doi: 10.1002/ca.20653, indexed in Pubmed: 18567019.
30. Maga A. Digital morphology: the final frontier. İstanbul Antropoloji Derg / Istanbul Anthropol Rev. 2022; 2: 45–59, doi: 10.26650/iar2022-1174374.
31. Mamidi A, Jyotsna G. The morphometric analysis of calcaneus and its articular facets. Indian J Clin Anat Physiol. 2022; 9(1): 22–24, doi: 10.18231/j.ijcap.2022.006.
32. Muthukumaravel N, Ravichandran D, Melani Rajendran S. Human calcaneal facets for the talus: patterns and clinical implications. J Clin Diagnostic Res. 2011; 5(4): 791–794.
33. Otağ İ, Tetiker H, Taştemur Y, et al. Morphometric Measurements of Calcaneus; Boehler'sangle and bone length estimation. Cumhuriyet Science Journal. 2017; 38(2): 256–256, doi: 10.17776/cumuscij.291995.
34. Prasad SA, Rajasekhar SS. Morphometric analysis of talus and calcaneus. Surg Radiol Anat. 2019; 41(1): 9–24, doi: 10.1007/s00276-018-2101-6, indexed in Pubmed: 30196483.
35. Sengodan V, Amruth KH. Bohler's and Gissane angles in the Indian population. Journal of Clinical Imaging Science. 2012; 2: 77, doi: 10.4103/2156-7514.104310.
36. Rokaya PK, Pokharel RK, Lamichhane AP. Radiographic evaluation of Calcaneal angles in patients presenting to tertiary care center of Nepal. J Inst Med Nepal. 2016; 38(2&3): 33–36, doi: 10.59779/jiomnepal.871.
37. Seyahi A, Uludağ S, Koyuncu LO, et al. The calcaneal angles in the Turkish population. Acta Orthop Traumatol

Turc. 2009; 43(5): 406–411, doi: 10.3944/AOTT.2009.406, indexed in Pubmed: 19881321.
38. Shoukry F, Aref Y, Sabry A. Evaluation of the normal calcaneal angles in Egyptian population. Alexandria J Med. 2019; 48(2): 91–97, doi: 10.1016/j.ajme.2011.07.001.
39. Singh DV. Assessment of morphometric study of calcaneus and its articular facets. Int J Acad Med Pharm. 2023; 5(1): 801–803, doi: http://dx.doi.org/10.47009/jamp.2023.5.1.166.
40. SK C, ST S, RN W. Pattern of talar articular facet of human calcaneum bone. IOSR J Dent Med Sci. 2014; 13(8): 16–18, doi: 10.9790/0853-13811618.
41. Uygur M, Atamaz F, Celik S, et al. The types of talar articular facets and morphometric measurements of the human calcaneus bone on Turkish race. Arch Orthop Trauma Surg. 2009; 129(7): 909–914, doi: 10.1007/s00402-008-0729-0, indexed in Pubmed: 18810474.
42. Velazquez ER, Parmar C, Jermoumi M, et al. Volumetric CT-based segmentation of NSCLC using 3D-slicer. Sci Rep. 2013; 3: 3529, doi: 10.1038/srep03529, indexed in Pubmed: 24346241.
43. Vučinić N, Teofilovski-Parapid G, Erić M, et al. Morphometric analysis of the patterns of calcaneal facets for the talus in Serbian population. PLoS One. 2020; 15(10): e0240818, doi: 10.1371/journal.pone.0240818, indexed in Pubmed: 33119596.
44. Yıldız K, Çetin T. Boehler-Gissane angles in patients who admitted to our hospital: how are Boehler and gissane angles in feet with pes planus? Kafkas J Med Sci. 2019; 9(3): 180–184, doi: 10.5505/kjms.2019.60362.
45. Zhang Q, Yeh HY. A comparative study on the tibial morphology among several populations in ancient East Asia. Elem Sci Anthr. 2021; 9(1), doi: 10.1525/elementa.2021.00071.